analytical chemistry

ARTICLE

pubs.acs.org/ac

Fourier Transform Infrared and Raman Spectroscopies for the Rapid Detection, Enumeration, and Growth Interaction of the Bacteria *Staphylococcus aureus* and *Lactococcus lactis* ssp. *cremoris* in Milk

Nicoletta Nicolaou, Yun Xu, and Royston Goodacre*

School of Chemistry and Manchester Interdisciplinary Biocentre, The University of Manchester, 131 Princess Street, Manchester M1 7DN, United Kingdom

Supporting Information

ABSTRACT: *Staphylococcus aureus* is one of the main pathogenic microorganisms found in milk and dairy products and has been involved in bacterial foodborne outbreaks in the past. Current enumeration techniques for bacteria are very time-consuming, typically taking 24 h or longer, and bacterial antagonism in the form of lactic acid bacteria (LAB) may inhibit the growth of *S. aureus*. Therefore, the aim of this investigation was to establish the accuracy and sensitivity of rapid nondestructive metabolic fingerprinting techniques, such as Fourier transform infrared (FT-IR) spectroscopy and Raman spectroscopy (RS), in combination with multivariate analysis techniques, for the detection and enumeration of *S. aureus* in milk, as well as to study the growth interaction between *S. aureus* and *Lactococcus lactis* ssp. *cremoris*, a common LAB. The two bacterial species were investigated both in a pure monoculture and in a combined inoculated coculture after inoculation into ultraheated milk during the first 24 h of growth at 37 °C. Plating techniques were used to obtain primary reference data for viable bacteria counts. Principal component discriminant function analysis, canonical correlation analysis, partial least-squares (PLS), and kernel PLS (KPLS) multivariate statistical techniques were employed to analyze the data. FT-IR provided very reasonable quantification results both with PLS and KPLS, the latter providing marginally better predictions, with correlation coefficients in the test set (Q^2) and training set (R^2) varying from 0.64 to 0.76 and from 0.78 to 0.88 for different bacterial sample combinations. RS results were less encouraging with high degrees of error and poor correlation to viable bacterial counts. *S. aureus* growth was not inhibited by the presence of the LAB, but metabolic fingerprinting of the coculture indicated that the phenotype of this dual bacterial culture was closer to that of pure LAB cultures. In conclusion, FT-IR spectroscopy in combination with the above multivariate techniques appears to be a promising discrimination and enumeration analytical technique for the two bacterial species. In addition, it has been demonstrated that the *L. cremoris* metabolic effect in milk dominates that of *S. aureus* even though there was no growth antagonism observed.

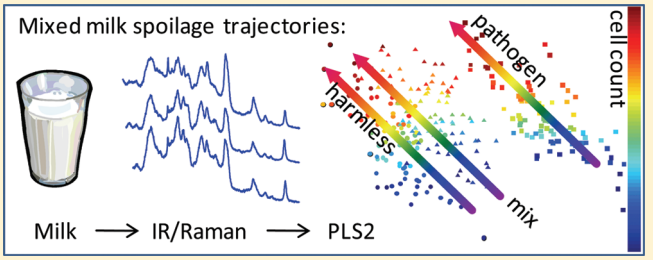

Foodborne diseases are a growing problem affecting food safety and quality and are becoming a major threat to public health with additional negative financial consequences to the dairy industry.[1] *Staphylococcus aureus* is a Gram-positive bacterium[2,3] commonly implicated in bacterial foodborne outbreaks, found mainly in the milk of animals suffering from mastitis,[4,5] and one of the main pathogens in milk and dairy products.[6−11]

With an optimal pH, water activity, and nutrients, milk appears to be a very good growth medium for *S. aureus*, being especially favorable to its growth at temperatures between 7 and 48 °C.[2,12−14] Strict regulation therefore exists internationally in regard to the levels of *S. aureus* present in raw cows' milk intended for human consumption or products made from raw milk without heat processing (due to the potential presence of heat-resistant staphylococcal enterotoxins[15−18]). A 2×10^3 cfu/mL concentration is set as the maximum limit allowed in the European Union, while identification of specific strains in milk leads to the direct withdrawal of that milk batch from the market (e.g., EC 2073/2005,[19] Council Directive 92/46/EEC[20]).

The current gold standard for the detection and enumeration of *S. aureus* at the industrial level, also used in ISO 6888-1, is the microbiological plate counting technique using Baird−Parker agar.[21] However, this method is too time-consuming, requiring at least 48 h for results, at which point the product may have already been released to the market. Latex agglutination tests available in the market are also time-consuming and also give retrospective answers as they require 20−24 h per sample.[22,23]

Polymerase chain reaction (PCR) techniques have also been investigated.[24−26] These methods are faster than immunological techniques with good detection limits of 100 cfu/g,[27,28] reaching 1 cfu/mL or cfu/g with 10 h of preprocessing.[29] The disadvantages of PCR techniques though include a high initial equipment cost, a constant need for highly trained stuff, and a risk of cross-contamination. Interference and inhibition from foodstuff also

Received: April 6, 2011
Accepted: June 3, 2011
Published: June 03, 2011

increase the requirement for additional processing and costs for purification and DNA isolation. Moreover, as DNA may be present from dead cells, PCR does not give an accurate measure of microbial viability. There is clearly a need for more rapid enumeration techniques that give immediate results.

Fourier transform infrared (FT-IR) spectroscopy is a biochemical fingerprinting technique, which in combination with multivariate statistical techniques has been shown to be a very fast and reasonably accurate method for bacterial detection and enumeration in milk.[30] Raman spectroscopy (RS) is also a nondestructive method requiring minimal sample preparation that can be considered to be complementary to FT-IR spectroscopy.[31,32] Both methods are powerful metabolic fingerprinting methods as they reflect accurately the phenotype of a sample, including changes to its metabolism.[33,34]

Bacterial antagonism is one of the factors influencing the growth of *S. aureus* in milk and dairy products. It appears that the presence of bacterial competitors can inhibit the growth of *S. aureus* due to changes in the substrate conditions, such as reduction in pH, production of volatile compounds, H_2O_2, or direct competition for nutrients.[35] The presence of high numbers of lactic acid bacteria (LAB) in raw milk or dairy products such as yogurt and cheese has been shown to inhibit the growth of *S. aureus* and the production of staphylococcal enterotoxins even at *S. aureus* levels of 10^3-10^5 cfu/mL or cfu/g.[18,36−38]

Lactococcus lactis ssp. *cremoris* is one of the homofermentative lactic acid bacteria incorporated in starter cultures involved in the production of a number of fermented milk products such as cheeses, buttermilk, and sour cream, with a particular effect on the flavor and texture of these products.[39] The effect of this commonly used LAB on the growth of *S. aureus* in milk has not been investigated in the past.

The aim of our study was therefore to investigate FT-IR and RS in combination with multivariate analytical techniques for the detection and enumeration of *S. aureus* and *L. cremoris* in milk. In addition, the use of these techniques will be employed in investigating the growth interaction between *S. aureus* and *L. cremoris* in inoculated milk.

MATERIALS AND METHODS

Bacterial Growth in Milk. The details, maintenance, and sample preparation of the bacteria are provided in the Supporting Information. The ultraheated (UHT) milk used in this experiment was purchased from a national retail outlet in the form of three 500 mL cartons of whole UHT milk with the same use-by date. Three 1 L sterile flasks containing 500 mL of whole UHT milk were inoculated, the first with *S. aureus*, the second with *L. cremoris*, and the third with both *S. aureus* and *L. cremoris* and placed in a rotational incubator at 37 °C and 200 rpm. Over the 24 h growth period, samples were then taken at 0, 60, 120, 150, 180, 210, 240, 300, 360, 420, 480, 720, 960, and 1440 min from all flasks. Samples of 1 mL were obtained at each time point from every flask and mixed in 9 mL of physiological saline (0.9%) for 1 min. The viable bacteria from each strain were then determined using a classical microbiological plating method. The latter involved an initial dilution series and lawning of the bacterial suspensions on tryptone soya agar (TSA; Oxoid, Hampshire, U.K.) plates in triplicate with 100 μL of homogeneous sample. The plates were then incubated for 20 h at 37 °C. and the viable bacteria were recorded as colony-forming units. When the two bacteria grow on TSA, they produce different types of colonies that differ in their shape, size, and color. Therefore, they can be readily differentiated on the basis of visualization.

Samples of 2 mL of milk were also collected at the same time points from each flask, divided into 1 mL volumes, and preserved at −80 °C. These aliquots were subsequently used for the FT-IR and Raman analyses. The entire experiment was repeated three times within a 30 day period.

FT-IR High-Throughput (HT) Spectroscopy. FT-IR analyses were undertaken on a Bruker Equinox 55 IR spectrometer using a deuterated triglycerine sulfate (DTGS) detector (Bruker Ltd., Coventry, U.K.) employing a motorized microplate module HTS-XT.[30] The previously frozen samples at −80 °C were slowly defrosted in ice, and each sample was mixed with the aid of a rotational mixer for 1 min. A 3 μL portion from each sample was then placed onto a ZnSe sample carrier, and sample drying was performed in an oven at 50 °C for 30 min. Samples were spread thinly over the surface in predetermined locations so that the whole of the IR beam interrogation area (ca. 1 mm diameter) was covered by the sample. Sample analysis was in a randomized order, and three replicate samples from each original sample were analyzed. As in previously described experiments,[30,40] the wavenumber used for these experiment was in the mid-IR range of 4000−600 cm^{-1}, 64 scans were coadded and averaged, and spectral resolution was 4 cm^{-1}. A total of 378 spectra were collected overall, with an individual spectrum collection time of approximately 30 s.

Raman Spectroscopy. Raman analysis was performed using a Renishaw 2000 Raman microscope with a 785 nm diode laser delivering typically ∼2 mW on the sample via a 50× objective.[41,42] The 785 nm wavelength was used for excitation as fluorescence interference is reduced when biological materials are analyzed. The GRAMS WIRE software was employed for instrument control and data collection. The samples were defrosted in ice and mixed for 1 min, and 1 μL from each sample was placed on a stainless steel plate. The plates were then dried at room temperature for 3 h; although for practical reasons drying was different compared to that for FT-IR spectroscopy, we have not observed any temperature-dependent effects on the Raman fingerprints. Collection of Raman spectra was performed in static mode over the wavenumber shift range of 400−2000 cm^{-1}. Three replicates were analyzed from each sample, with a total of 378 spectra collected, from the different time points of bacterial growth in milk. The total integration time for each sample was 3 min.

Preprocessing. ASCII data were exported from the Opus software used to control the FT-IR instrument and imported into Matlab version Seven (The Mathworks, Inc., Matick, MA). Similarly, the ASCII data from the Raman instrument were also imported into Matlab version Seven, and both sets of data were preprocessed using a standard normal variate (SNV).[43−45] Multivariate statistical methods such as cluster analysis and supervised regression-based techniques, partial least-squares (PLS) and kernel PLS (KPLS), were subsequently used to explore the relationship between the FT-IR and Raman spectra and the number of viable bacteria in milk.

Cluster Analysis. Cluster analysis was performed in two steps as has been fully described elsewhere.[46] The first step involved the use of principal component analysis (PCA). This statistical process transforms potentially correlated variables into a smaller number of uncorrelated variables called principal components (PCs). PCA identifies data patterns and highlighting differences and similarities and results in a significant reduction in the number of dimensions needed to describe these multivariate data while maintaining the majority of the original variance.[47] In the second

step, discriminant function analysis (DFA) was used. This is a statistical process which employs prior knowledge of which spectra are machine replicates and uses this information to discriminate data on the basis of the PCs. As machine replicates are used, this does not bias the cluster analysis in any way.

Supervised Analysis. In this process the knowledge of both input values, such as the FT-IR spectra, and target/output values, such as those derived from the bacterial counts (as log values), are used during calibration. This results in an association model between inputs and outputs. The linear regression analysis technique PLS and the nonlinear regression method KPLS were used in this experiment, along with canonical correlation analysis (CCA).

Validation of PLS and KPLS is an important aspect of these analyses because of the great power of supervised analysis methods. To perform this validation, for each of the three bacterial combinations (two single and one double), 70% of the total spectra were randomly selected as the training set and the remaining 30% were used as the test set. This selection and test process was repeated four times, and the average model values were calculated.

CCA,[48] PLS,[49] and KPLS[50] were performed exactly as reported by us elsewhere.[40,51] All algorithms were programmed in Matlab version Seven and model validation, latent variable selection, and prediction errors calculated as described and detailed above.

RESULTS AND DISCUSSION

Viable Counts (VCs). Results from the experiments involving *S. aureus* both when inoculated in isolation in UHT milk at 37 °C and when inoculated in combination with *L. cremoris* are illustrated in Tables S1 and S2 (Supporting Information) and are described further below. As can be seen from the growth curves (Figure S1, Supporting Information), the initial bacterial inoculation numbers for *S. aureus* were very similar with mean log(VC) values of 5.20 and 5.72 for the pure inoculant and the coculture, respectively, the latter being analogous to the initial bacterial inoculation numbers of *L. cremoris* in the coculture (mean log(VC) of 5.67, Table S2). The lag phase of *S. aureus* growth in both experiments appeared to be from 0 to 120 min, with mean log(VC) values of 5.20−5.49 and 5.72−5.96 for pure and coculture inoculations, respectively. The exponential growth phase initiated at 120 min and ended at ∼480 min with mean log(VC) values of 5.49−8.03 (in pure culture) and 5.96−7.81 (in coculture). The stationary phase commenced thereafter, and the final mean log(VC) values were 8.26 and 8.17 after 1440 min (24 h) of growth for monoculture and coculture inoculations, respectively. The bacterial growth curves for *L. cremoris* both in pure culture and in coculture are also shown in Figure S1 and show dynamics very similar to those described above for *S. aureus* (see Table S2). There was certainly no indication that the presence of *L. cremoris* in the mixture samples interfered in any way with the growth of *S. aureus*, although the growth of *L. cremoris* in the presence of *S. aureus* did appear to be impeded with a lower final bacterial count at 24 h of 7.96 (log(VC)) compared to 9.05 in the pure culture.

FT-IR and Raman Data. Plating and counting bacteria is slow as overnight incubations are needed and selective media required; therefore, we investigated whether vibrational spectroscopy could aid and help with coculturing. In infrared the molecular vibrations must cause a net change in the dipole moment of the molecule. By contrast, for a vibration to be Raman active, the polarizability of the molecule must change with the vibrational motion. Therefore, the spectra from each technique are expected to be different but complement each other.[32] Thus, both methods

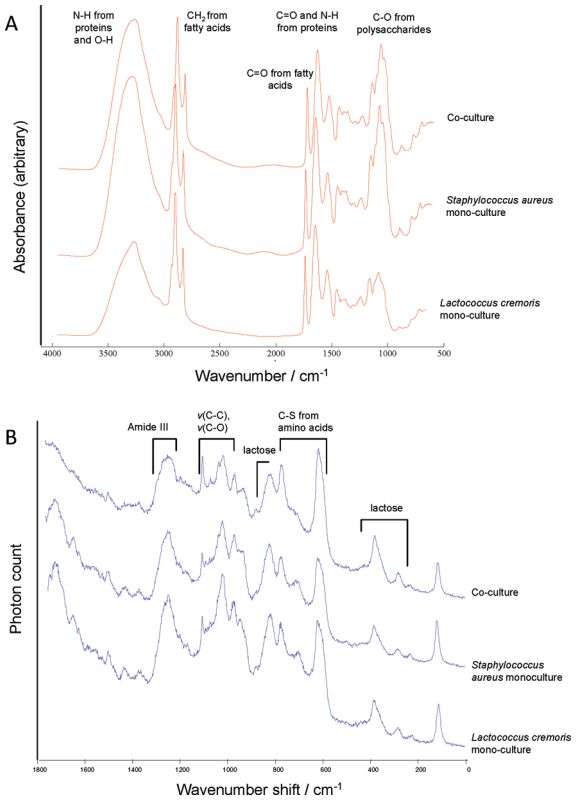

Figure 1. Typical (A) FT-IR HT and (B) Raman spectra at 480 min (6 h) for *S. aureus* and *L. cremoris* after inoculation in UHT milk in monoculture and in coculture. Spectra are offset so that features can be observed.

were investigated for their abilities to generate meaningful metabolic fingerprints from the milk during bacterial growth.

Visual inspection of the spectra obtained using FT-IR HT spectroscopy for the two bacterial species in monoculture and in coculture only revealed some differences between spectra. Representative spectra from FT-IR HT spectroscopy at 480 min (6 h) are illustrated in Figure 1A. Several peaks appear to be of particular interest, namely, the peak at 3300 cm^{-1}, representing the peptide bonds ν(N−H) from proteins and ν(O−H), the peak at 1100 cm^{-1}, representing ν(C−O) from carbohydrates, and the clear ratio between the amide I bands at ∼1650 cm^{-1} from ν(C═O) with the carbohydrate (1100 cm^{-1}). Spectral absorption at 3300 and 1100 cm^{-1} appears to be lower during the growth of *L. cremoris* compared to the growth of *S. aureus*, and the ratio of amide I to polysaccharide is equivalent in *S. aureus* and the coculture, but for *L. cremoris* the amide I:polysaccharide ratio is significantly greater. This represents different metabolic potentials of these organisms with the higher rate of carbohydrate utilization by the fermentative metabolism of *L. cremoris*. Representative spectra derived from Raman spectroscopy at 480 min (6 h) for both bacteria in isolation and from the combined mixture are shown in Figure 1B. These Raman spectra appear to be almost identical with no apparent differences on visual inspection. Higher intensity of two peaks can be seen in the combined mixture spectrum at the 1110 cm^{-1} ν(C−C) mode and the 610 − 630 cm^{-1} ν(C−S) mode, both representing amino acids. The remaining prominent peaks in all spectra appear at the 1230−1290 cm^{-1} amide III mode, 1050−920 cm^{-1} ν(C−C) and ν(C−O) modes, 760−790 cm^{-1} ν(C−S) mode representing various amino acids, and 810−850, 380−400, and 280−300 cm^{-1} modes representing lactose.[52−54]

dx.doi.org/10.1021/ac2008256 |*Anal. Chem.* 2011, 83, 5681–5687

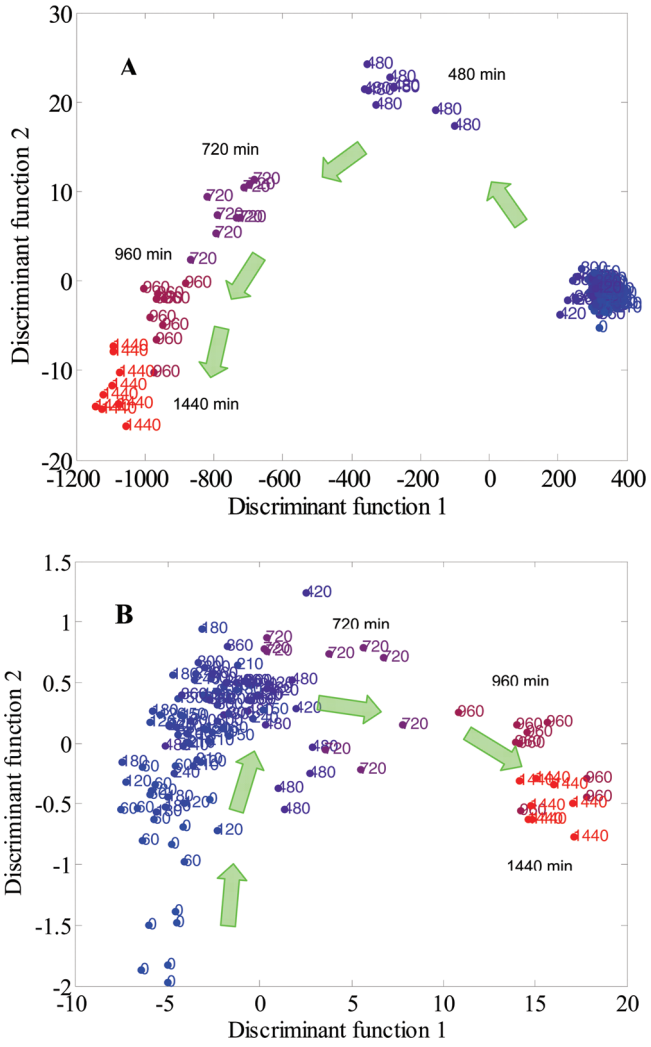

Figure 2. PC-DFA plot of (A) FT-IR HT spectra and (B) Raman spectra for *L. cremoris* during monoculture in UHT milk. PCs 1−20 (accounting for (A) 99.93% and (B) 98.44% of the total variance) were used by the DFA algorithm with a priori knowledge of machine replicates (i.e., 1 class per time point, giving 14 classes in total). Each different color represents a distinct time point, and block arrows indicate the trend of the data.

Trajectory Analysis. Cluster analysis using PC-DFA was subsequently performed in an attempt to gain more information regarding potential differences between the milk sustaining bacterial growth from the FT-IR and Raman spectra. As an example, the PC-DFA results from FT-IR HT data on the *L. cremoris* monocultures are shown in Figure 2A. This trajectory plot indicates that after 420 min there is a clear distinction between time points in the PC-DFA space. Samples collected from 720 to 1440 min followed a downward left trajectory, and the mean log(VC) values increase from 8.14 to 8.26, suggesting that while there is very little growth, the fingerprint of the milk during this time period is changing in a particular manner.

The same general trend is also seen in the PC-DFA space from the Raman data collected from the same bacteria (Figure 2B), with the additional good distinction between time points at 0 min as well as those after 480 min. However, the spread of these points is much greater in this analysis compared to the PC-DFA FT-IR HT analysis for the same bacteria. This more diffuse clustering of the individual time points suggests that there was a lack of precision in spectral collection.

Similar findings were obtained for the other monoculture (*S. aureus*) as well as for the coculture for both FT-IR and Raman data (data not shown). Overall these trajectory analyses showed that sample distinction was possible only after the initiation of the stationary phase (after 480 min of growth) for both bacterial species and the coculture. By contrast, the spectra collected from the lag and exponential phases for all three cultures appeared to be very similar as samples collected from 0 to 420 min were coincident in PC-DFA space, despite this being when most growth occurred; typically log(VC) increased from ~5.2 to ~7.5.

Table 1. Canonical Correlation Coefficient (R) Values for FT-IR and Raman Data for *S. aureus* and *L. cremoris* Monocultures and Cocultures against VC and Time

	FT-IR R		Raman R	
	VC	time	VC	time
S. aureus monoculture	0.75	0.95	0.81	0.94
L. cremoris monoculture	0.73	0.96	0.82	0.93
S. aureus in coculture	0.86	0.98	0.75	0.95
L. cremoris in coculture	0.86	0.98	0.79	0.95

Canonical Correlation Analysis. To investigate these spectral changes further, CCA was performed on the FT-IR and Raman data obtained for the two organisms in monoculture and in coculture. Canonical correlation coefficients (R) of the various plots of canonical variable against VC and time are shown in Table 1, and CCA plots for *S. aureus* in pure and mixed cultures are shown in Figure S2 (Supporting Information). Visual inspection of these results indicates the presence of a linear pattern in the bacterial concentration levels with the FT-IR and Raman data and that the correlation coefficients appear to be better when calculated against time rather than against VC. For correlations with time both FTIR and Raman data show better results in the co-cultures (Table 1). Although the CCA was better with respect to time, correlations between ~0.73 and ~0.86 were found for all bacteria with respect to VCs. As microbiologists would prefer to have estimates of bacterial numbers rather than growth time, these results do suggest that further chemometric analysis should be performed to effect bacterial quantification from these vibrational spectroscopic data.

Bacterial Quantification. Quantification of each bacterial species was attempted using linear PLS and nonlinear KPLS regression as described in previous work.[40] Each model was constructed using 70% of the values as the training set and the remaining 30% for the test set. Four different models were constructed using different combinations of spectra in the training and test sets, and these results were combined to obtain the average prediction statistics. Only data collected from the first 480 min of the experiments were used as the bacterial growth curves (Figure S1, Supporting Information) demonstrate very little growth after the stationary phase is reached. Figure 3 illustrates two representative PLS models predicting *S. aureus* numbers from FT-IR data from pure cultures of *S. aureus* (Figure 3A) and cocultures with *L. cremoris* (Figure 3B). Table 2 shows the mean and standard deviation values for each bacterial species in the different growth environments analyzed by both PLS and KPLS.

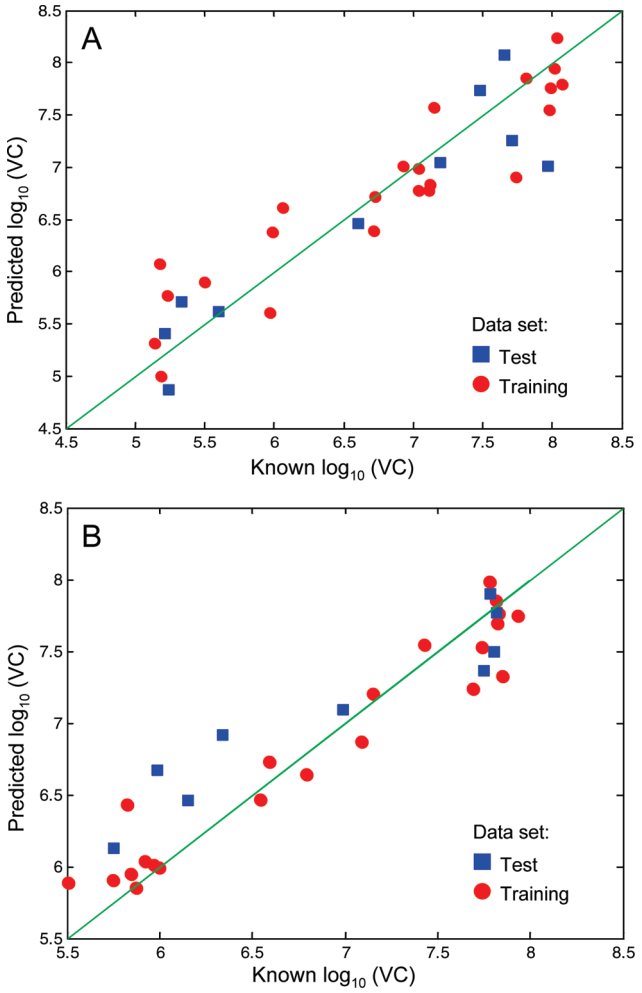

Figure 3. Representative plots illustrating the average predicted VC values (log) derived from PLS against the average measured VC values (log) measured with FT-IR HT for *S. aureus* (A) monoculture and (B) coculture. For (A), the Q^2 value for the test set was 0.68 and the R^2 value for the training set was 0.79, with RMS errors (log) for the calibration and prediction of 0.46 and 0.61, respectively. Ten PLS factors were used for this model. For (B), the Q^2 value for the test set was 0.69 and the R^2 value for the training set was 0.84, with RMS errors (log) for the calibration and prediction of 0.35 and 0.47, respectively. Three PLS factors were used for this model.

For analysis of the three cultures using FT-IR spectroscopy, both PLS and KPLS appeared to have good and similar predictive values for both bacteria (Table 2). In the PLS models the root-mean-square error of the training set (RMSEC) appeared to vary from log 0.25 to log 0.52, with RMS errors in the independent set (RMSEP) from log 0.38 to log 0.59. The correlation coefficients in the test set (Q^2) and training set (R^2) varied on average from 0.64 to 0.76 and from 0.78 to 0.88, respectively. KPLS yielded comparable values with RMSEC from log 0.26 to log 0.36 and RMSEP from log 0.40 to log 0.59; the Q^2 variation was from 0.69 to 0.720, and the R^2 average values were from 0.81 to 0.87. Overall, it appeared that the prediction of *L. cremoris* in the coculture provided a marginally better predictive model in both PLS and KPLS. By contrast, when the Raman spectra were analyzed with PLS and KPLS in exactly the same way as the FT-IR data, the predictions of the viable bacterial load in UHT milk were not satisfactory, with large RMSEPs (typically log 1.2) and RMSECs (typically log 0.75); therefore, these statistics are not included in Table 2.

Table 2. Comparison of the PLS Regression and the Nonlinear KPLS Results of the FT-IR HT Spectra for Determining the Number of Viable Bacteria in UHT Milk[a]

	PLS		KPLS	
	mean	SD	mean	SD
S. aureus Monoculture				
RMSECV	0.63	0.08	0.61	0.08
RMSEC	0.52	0.19	0.36	0.06
RMSEP	0.47	0.10	0.59	0.06
correlation coefficient in the training set (R^2)	0.78	0.14	0.87	0.04
correlation coefficient in the test set (Q^2)	0.74	0.09	0.69	0.02
L. cremoris Monoculture				
RMSECV	0.65	0.06	0.65	0.06
RMSEC	0.26	0.03	0.26	0.03
RMSEP	0.59	0.07	0.59	0.07
correlation coefficient in the training set (R^2)	0.88	0.02	0.81	0.13
correlation coefficient in the test set (Q^2)	0.64	0.07	0.71	0.14
S. aureus in Coculture				
RMSECV	0.44	0.03	0.44	0.03
RMSEC	0.37	0.02	0.36	0.02
RMSEP	0.47	0.06	0.47	0.05
correlation coefficient in the training set (R^2)	0.81	0.02	0.82	0.01
correlation coefficient in the test set (Q^2)	0.70	0.03	0.70	0.03
L. cremoris in Coculture				
RMSECV	0.32	0.01	0.34	0.01
RMSEC	0.25	0.03	0.29	0.03
RMSEP	0.38	0.06	0.40	0.04
correlation coefficient in the training set (R^2)	0.87	0.03	0.82	0.03
correlation coefficient in the test set (Q^2)	0.76	0.04	0.72	0.07

[a] RMSECV represents the root mean square error for the cross-validation, RMSEC the root mean square error for the calibration, and RMSEP the root mean square error for the predictions produced for the independent test set. SD stands for standard deviation.

PLS2 Projection Analysis. To investigate whether the metabolic fingerprints from the cocultured samples were closer to one of the pure cultures, a PLS2 model was first built on the combined data set from the two monocultures. In the response matrix **Y**, one column was allocated to the VCs from *L. cremoris* and the other column for the *S. aureus* counts, with the corresponding elements in **Y** set to zero. That is to say, if log(VC) for *S. aureus* were 5.7, then the target response vector in **Y** would be [5.7 0], while if log(VC) for *L. cremoris* were 7.8, it would be [0 7.8]. In this way, the PLS model was "forced" to focus on the *unique* features of

dx.doi.org/10.1021/ac2008256 |*Anal. Chem.* 2011, 83, 5681–5687

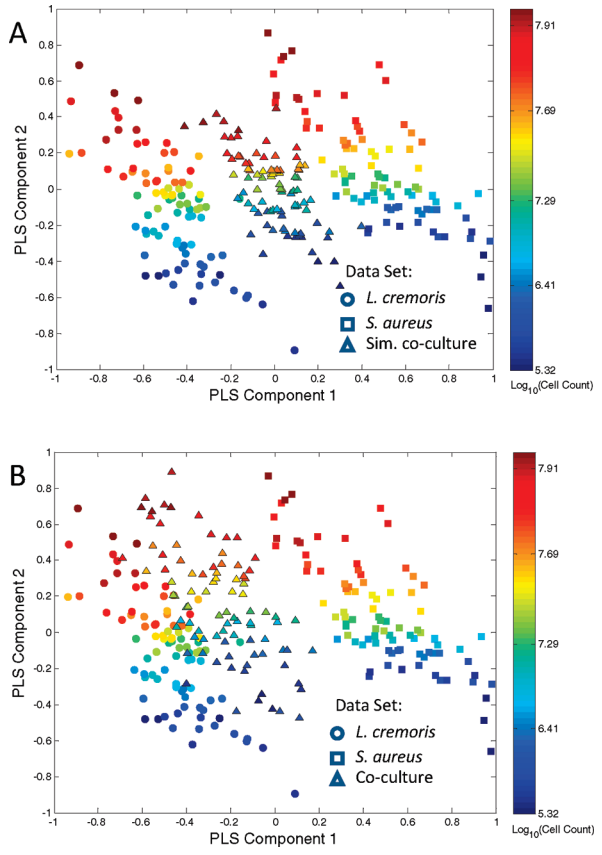

Figure 4. PLS2 models calibrated with pure monocultures of *S. aureus* and *L. cremoris* with (A) simulated cultures and (B) coculture samples projected into the PLS2 model. Colors represent log(cell counts), and the symbols represent the different cultures or simulated data.

each bacterium and actively penalize the common features modeling the cell growth. If the coculture samples were "dominated" by one type of bacterium, then after projection into this model, the PLS scores would be more overlapping with those of the "dominating" bacterium.

To test this hypothesis, "simulated" coculture spectra were generated by averaging a series from the two pure bacterial spectra; i.e., each spectrum in the simulated coculture was the mean of the two pure bacterial spectra which had similar VCs at the same time points. If the previous assumptions in the PLS2 projections were correct, then the scores of this simulated coculture would appear in the middle of the two pure bacterial samples. Figure 4A shows the simulated data projected into PLS2 latent variable space, and it can indeed be seen that the simulated data appear in the middle of the valley between the two pure bacterial cultures. Note that the two pure cultures are separated but split in both PLS components 1 and 2 and the direction indicated by the coloring represents the increase in VC.

Figure 4B illustrates the PLS2 projection of the real spectra from the cocultures, and rather than falling between the two bacteria, these data are clearly located closer to the pure *L. cremoris* spectra. This shows that the metabolic fingerprint is dominated by *L. cremoris* in the coculture rather than the *S. aureus* phenotype. Another indication that the coculture is closer to the pure *L. cremoris* is that when the **Y** predictions are inspected from the PLS2 model (data not shown), the residuals of the predictions are lower for *L. cremoris* compared to *S. aureus*. All the cell counts for *S. aureus* have been seriously underestimated and are close to zero, whereas the estimates for *L. cremoris* were the same as for *L. cremoris* from the coculture.

CONCLUDING REMARKS

In contrast to Raman spectroscopy, the metabolic fingerprinting revealed through FT-IR HT spectroscopy was able to give reasonably good estimates of the levels of *S. aureus* and *L. cremoris* in both pure and cocultures when these bacteria were grown in UHT milk.

While in the literature the growth of LAB in milk has been reported to slow the growth of pathogens, including *S. aureus*,[55,56] from the growth curve analysis (Figure S1, Supporting Information), we certainly did not see any antagonism on *S. aureus* when grown with *L. cremoris*; if anything, the opposite was true in that the growth of *L. cremoris* was slightly lower when cultured with *S. aureus*. The latter may be of particular importance in the dairy industry, especially in the manufacture of products using unpasteurized raw milk and LAB, such as cheese and butter.

Interestingly, when the phenotype of the coculture was compared to those from the pure cultures of bacteria in UHT milk using PLS2 (Figure 4), despite the reduction in the growth of *L. cremoris*, this phenotype did appear to dominate the coculture. This may be due to the fact that this LAB has a fermentative metabolism where sugars from the milk are fermented to organic acids, which will lower the pH of the milk and cause additional phenotypic changes in the milk substrate, such as curdling of the proteins.

In conclusion, we have demonstrated that FT-IR spectroscopy when combined with chemometrics is a powerful approach for bacterial enumeration in milk and gives results in a few minutes, rather than in several days, which is typical of classical methods used in the industry. Moreover, this is the first demonstration that FT-IR can perform enumeration of bacteria in cocultures without the need for their prior separation.

ASSOCIATED CONTENT

Supporting Information. Additional information as noted in text. This material is available free of charge via the Internet at http://pubs.acs.org.

AUTHOR INFORMATION

Corresponding Author

*E-mail: roy.goodacre@manchester.ac.uk.

ACKNOWLEDGMENT

Y.X. and R.G. acknowledge the Symbiosis-EU (www.symbiosis-eu.net) project (Grant 211638) financed by the European Commission under the 7th Framework Programme for Research and Technological Development. The information in this document reflects only the authors' views, and the Commission is not liable for any use that may be made of the information contained herein.

REFERENCES

(1) World Health Organization, Geneva, Switzerland, 2010.

(2) Adams, M. R.; Moss, M. O. *Food Microbiology*, 2nd ed.; The Royal Society of Chemistry: Cambridge, U.K., 2000.

(3) Jablonski, L. M.; Bohach, G. A. In *Food Microbiology: Fundamentals and Frontiers*, 2nd ed.; Doyle, M. P., Beuchat, L. R.,

Montville, T. J., Eds.; ASM Press: Washington, DC, 2001; pp 411−434.
(4) Bergdoll, M. S. In *Foodborne Bacterial Pathogens*; Doyle, M. P., Ed.; Marcel Dekker: New York, 1989; pp 463−523.
(5) Gilmour, A.; Harvey, J. *J. Appl. Bacteriol. Symp.* **1990**, Suppl. 19, 147S−166S
(6) Balaban, N.; Rasooly, A. *Int. J. Food Microbiol.* **2000**, *61*, 1–10.
(7) World Health Organization (WHO). 7th Report; WHO: Geneva, Switzerland, 1993−1998.
(8) Asao, T.; Kumeda, Y.; Kawai, T.; Shibata, T.; Oda, H.; Haruki, K.; Nakazawa, H.; Kozaki, S. *Epidemiol. Infect.* **2003**, *130*, 33–40.
(9) Bayser, M. L. D.; Dufour, B.; Maire, M.; Lafarge, V. *Int. J. Food Microbiol.* **2001**, *67*, 1–17.
(10) Ostyn, A.; Buyser, M. L. D.; Guillier, F.; Groult, J.; Felix, B.; Salah, S.; Delmas, G.; Hennekinne, J. A. *Eurosurveillance* **2010**, *15*, 19528.
(11) Schmid, D.; Fretz, R.; Winter, P.; Mann, M.; Hoger, G.; Stoger, A.; Ruppitsch, W.; Ladstatter, J.; Mayer, N.; Martin, A. d.; Allenberger, F. *Wien. Klin. Wochenschr.* **2009**, *121*, 125–131.
(12) Qi, Y.; Miller, K. J. *J. Food Prot.* **2000**, *63*, 473–478.
(13) Schmitt, M.; Schuler-Schmidt, U.; Schmidt-Lorenz, W. *Int. J. Food Microbiol.* **1990**, *11*, 1–20.
(14) Clark, W. S.; Nelson, F. E. *J. Dairy Sci.* **1961**, *44*, 232–236.
(15) Jarraud, S.; Peyrat, M. A.; Lim, A.; Tristan, A.; Bes, M.; Lougel, C.; Etienne, J.; Vanedesch, F.; Bonneville, M.; Linal, G. *J. Immunol.* **2001**, *166*, 669–677.
(16) Letertre, C.; Perelle, S.; Dilasser, F.; Fach, P. *J. Appl. Microbiol.* **2003**, *95*, 38–43.
(17) Ono, H. K.; Omoe, K.; Imanishi, K.; Iwakabe, Y.; Hu, D. L.; Kato, H.; Saito, N.; Nakane, A.; Uchiyama, T.; Shinagawa, K. *Infect. Immun.* **2008**, *76*, 4999–5005.
(18) Scientific Committee on Veterinary Measures Relating to Public Health (SCVPH), Brussels, Belgium, 2003; Vol. *2010*.
(19) The Commission of the European Communities, Brussels, Belgium, 2005.
(20) The Council of the European Communities, Brussels, Belgium, 1992.
(21) Baird-Parker, A. C. *J. Appl. Bacteriol.* **1962**, *25*, 12–19.
(22) Akkaya, L.; Sancak, Y. C. *Bull. Vet. Inst. Pulawy* **2007**, *51*, 401–406.
(23) Rose, S. A.; Bankes, P.; Stringer, M. F. *Int. J. Food Microbiol.* **1989**, *8*, 65–72.
(24) Ahmadi, M.; Rohani, S. M. R.; Ayremiou, N. *Comp. Clin. Pathol.* **2010**, *19*, 91–94.
(25) Hein, I.; Jorgensen, H. J.; Loncarevic, S.; Wagner, M. *Res. Microbiol.* **2005**, *156*, 554–563.
(26) Graber, H. U.; Casey, M. G.; Naskova, J.; Steiner, A.; Schaeren, W. *J. Dairy Sci.* **2007**, *90*, 4661–4669.
(27) Cremonesi, P.; Perez, G.; Pisoni, G.; Moroni, P.; Morandi, S.; Luzzana, M.; Brasca, M.; Castiglioni, B. *Lett. Appl. Microbiol.* **2007**, *45*, 586–591.
(28) Tamarapu, S.; McKillip, J. L.; Drake, M. *J. Food Prot.* **2001**, *64*, 664–668.
(29) Chiang, Y. C.; Fan, C. M.; Liao, W. W.; Lin, C. K.; Tsen, H. Y. *J. Food Prot.* **2007**, *70*, 2855–2859.
(30) Nicolaou, N.; Goodacre, R. *Analyst* **2008**, *133*, 1424–1431.
(31) Ferraro, J. R.; Nakamoto, K. *Introductory Raman Spectroscopy*, 1st ed.; Academic Press: London, 1994.
(32) Goodacre, R.; Radovic, B. S.; Anklam, E. *Appl. Spectrosc.* **2002**, *56*, 521–527.
(33) Goodacre, R.; Vaidyanathan, S.; Dunn, W. B.; Harrigan, G. G.; Kell, D. B. *Trends Biotechnol.* **2004**, *22*, 245–252.
(34) Ellis, D. I.; Goodacre, R. *Analyst* **2006**, *131*, 875–885.
(35) Genigeorgis, C. A. *Int. J. Food Microbiol.* **1989**, *9*, 327–360.
(36) Lodi, R.; Malaspina, P.; Brasca, M. *Ind. Latte* **1994**, *30*, 3–16.
(37) Ortolani, M. B. T.; Yamazi, A. K.; Moraes, P. M.; Vicosa, G. N.; Nero, L. A. *Foodborne Pathog. Dis.* **2010**, *7*, 175–180.
(38) Cleveland, J.; Montville, T. J.; Nes, I. F.; Chikindas, M. L. *Int. J. Food Microbiol.* **2001**, *71*, 1–20.
(39) Johnson, M. E.; Steele, J. L. In *Food Microbiology: Fundamentals and Frontiers*, 2nd ed.; Doyle, M. P., Beuchat, L. R., Montville, T. J., Eds.; ASM Press: Washington, DC, 2001; pp 651−664.
(40) Nicolaou, N.; Xu, Y.; Goodacre, R. *J. Dairy Sci.* **2010**, *93*, 5651–5660.
(41) Jarvis, R. M.; Goodacre, R. *Anal. Chem.* **2004**, *76*, 40–47.
(42) Jarvis, R. M.; Law, N.; Shadi, I. T.; O'Brien, O.; Lloyd, J.; Goodacre, R. *Anal. Chem.* **2008**, *80*, 6741–6746.
(43) Barnes, R. J.; Dhanoa, M. S.; Lister, S. *J. Near Infrared Spectrosc.* **1993**, *1*, 185–186.
(44) Barnes, R. J.; Dhanoa, M. S.; Lister, S. J. *Appl. Spectrosc.* **1989**, *43*, 772–777.
(45) Dhanoa, M.; Lister, S.; Sanderson, R.; Barnes, R. J. *J. Near Infrared Spectrosc.* **1994**, *2*, 43–47.
(46) Goodacre, R.; Timmins, E. M.; Burton, R.; Kaderbhai, N.; Woodward, A. M.; Kell, D. B.; Rooney, P. J. *Microbiology* **1998**, *144*, 1157–1170.
(47) Goodacre, R. *Vib. Spectrosc.* **2003**, *32*, 33–45.
(48) Hotelling, H. *Biometrika* **1936**, *28*, 312–377.
(49) Martens, H.; Naes, T. In *Multivariate Calibration*, 1st ed.; John Wiley & Sons: Chichester, U.K., 1989; pp 73−236.
(50) Shawe-Taylor, J.; Christianini, N. *Kernel Methods for Pattern Analysis*; Cambridge University Press: Cambridge, U.K., 2004.
(51) Nicolaou, N.; Xu, Y.; Goodacre, R. *Anal. Bioanal. Chem.* **2010**, *399*, 3491–3502.
(52) Kirk, J. H.; Dann, S. E.; Blatchford, C. G. *Int. J. Pharm.* **2007**, *334*, 103–114.
(53) Li-Chan, E. C. Y. *Trends Food Sci. Technol.* **1996**, *7*, 361–370.
(54) McGoverin, C. M.; Clark, A. S. S.; Holroyd, S. E.; Gordon, K. C. *Anal. Chim. Acta* **2010**, *673*, 26–32.
(55) Fang, W.; Shi, M.; Huang, L.; Chen, J.; Wang, Y. *Vet. Res.* **1996**, *27*, 3–12.
(56) Radovanovic, R. S.; Katic, V. *Bulg. J. Agric. Sci.* **2009**, *15*, 196–203.